Published in final edited form as:

Science. 2013 February 8; 339(6120): 694–698. doi:10.1126/science.1229934.

Structural basis for hijacking of cellular LxxLL motifs by papillomavirus E6 oncoproteins

Katia Zanier[1,†], **Sebastian Charbonnier**[1,†], **Abdellahi Ould M'hamed Ould Sidi**[1], **Alastair G. McEwen**[2], **Maria Giovanna Ferrario**[2], **Pierre Poussin**[2], **Vincent Cura**[2], **Nicole Brimer**[3], **Khaled Ould Babah**[1], **Tina Ansari**[3], **Isabelle Muller**[1], **Roland H. Stote**[2], **Jean Cavarelli**[2,*], **Scott Vande Pol**[3,*], and **Gilles Travé**[1,*]

[1]Biotechnologie et signalisation cellulaire UMR 7242, Ecole Superieure de Biotechnologie de Strasbourg, Boulevard Sébastien Brant, BP 10413, F-67412 Illkirch, France

[2]Institut de Génétique et de Biologie Moléculaire et Cellulaire (IGBMC)/INSERM U964/CNRS UMR 7104/Université de Strasbourg, 1 rue Laurent Fries, BP 10142, F-67404 Illkirch, France

[3]Department of Pathology, University of Virginia, P.O. Box 800904, Charlottesville, Virginia 22908-0904, USA

Abstract

E6 viral oncoproteins are key players in epithelial tumors induced by Papillomaviruses in vertebrates, including cervical cancer in humans. E6 proteins target many host proteins by specifically interacting with acidic LxxLL motifs. Here, we solved the crystal structures of Bovine (BPV1) and Human (HPV16) Papillomavirus E6 proteins bound to LxxLL peptides from the focal adhesion protein paxillin and the ubiquitin ligase E6AP, respectively. In both E6 proteins, two zinc domains and a linker helix form a basic-hydrophobic pocket, which captures helical LxxLL motifs in a way compatible with other interaction modes. Mutational inactivation of the LxxLL binding pocket disrupts the oncogenic activities of both E6 proteins. This work reveals the structural basis of both the multifunctionality and the oncogenicity of E6 proteins.

Papillomaviruses (PV) infect the epithelia of vertebrates. More than 200 PV types have been identified (1), among which a subset is tumorigenic. Cervical cancers are caused by "high-risk" mucosal Human PVs (hrm-HPVs), of which HPV16 is the most prevalent and best studied type (2), whereas some skin cancers have been associated with "high-risk" cutaneous HPVs (3). Bovine Papillomavirus 1 (BPV1) also induces tumors in its natural host (cattle) and in horses (4).

PV carcinogenesis is primarily linked to two PV oncoproteins, E6 and E7. Hrm-HPV E6 recruits the ubiquitin ligase E6AP (5) and tumor suppressor p53, leading to ubiquitin–mediated degradation of p53 (6). E6 also interacts with many other cellular proteins related to cancer pathways (7, 8). Mucosal and cutaneous HPV E6 oncoproteins recognize some of their target proteins, including E6AP, the Interferon Regulatory Factor IRF-3 (9) and the Notch co-activator MAML1 (8, 10, 11) through acidic leucine-rich motifs containing the LxxLL consensus sequence (12, 13). BPV1 E6 recognizes a particular sub-class of acidic

*Correspondence to: gilles.trave@unistra.fr, vandepol@virginia.edu, cava@igbmc.fr.
†These authors contributed equally to this work

Author contributions

K.Z., S.C., N.B., A.o.M.o.S., T.A., K.o.B., I.M., A.G.mcE., P.P., V.C. and S.V.P. performed experiments; M.G.F. and R.H.S. performed computational analysis; J.C. and A. G. mcE. performed structure determination. S.C., K.Z., J.C., S.V.P. and G.T. analyzed the data. G.T., K.Z., S.C., S.V.P. J.C. and R.S. prepared the manuscript. G.T., S.V.P., J.C. and R.S. supervised the work.

LxxLL sequences, termed LD motifs, which mediate protein-protein interactions regulating cell motility, cell adhesion and gene expression (14). BPV1 E6 recognizes several LD motifs of the focal adhesion protein paxillin, and this interaction is required for cellular transformation (15, 16, 17). Despite their small size (about 150 residues), E6 proteins combine multiple interaction sites. For instance, hrm-HPV E6 interacts not only with LxxLL motifs but also with PDZ domains involved in cell polarity and adhesion (18), and also possesses a self-association interface required for the p53 degradation activity (19).

Mammalian PV E6 proteins are cysteine-rich proteins consisting of two zinc-binding domains named E6N and E6C. Whereas structures of isolated E6N and E6C domains have been determined (19, 20), full-length E6 proteins undergo self-oligomerization (21), which has precluded structural analysis.

To circumvent this problem, we applied two solubilizing strategies to the BPV1 and the HPV16 E6 proteins (22). For BPV1 E6, we fused a crystallization-prone mutant of the bacterial Maltose Binding Protein (MBP) to an E6-binding LxxLL sequence present in the paxillin LD1 motif that is known to solubilize E6 (23), and then to the BPV1 E6 protein (Supplemental Fig. 1A). The resulting MBP-LxxLL-E6 triple fusion protein purified as a soluble monomer and yielded crystals that diffracted at a resolution better than 2.3 Å (Supplemental Table 1). For HPV16 E6, we purified the monomeric E6 F47R 4C/4S mutant that combines the F47R mutation disrupting E6N dimerization, and four mutations at non-conserved cysteines preventing disulfide-mediated aggregation (19). Purified E6 F47R 4C/4S was mixed with equimolar amounts of an MBP-LxxLL fusion containing the E6-binding LxxLL sequence of E6AP (Supplemental Fig. 1B). The complex yielded crystals that diffracted at a resolution better than 2.6 Å (Supplemental Table 1). Both structures were solved by molecular replacement using the known structure of MBP as a template (Fig. 1 and Supplemental Fig. 2).

The overall structures of the two E6/LxxLL complexes are very similar (Supplemental Fig. 3A) despite low sequence identity (30%), suggesting that crystallization-promoting strategies did not introduce artifacts. Indeed, MBP is differently positioned relative to E6 in the two crystals (Supplemental Fig. 2) and the five solubilizing mutations of E6 F47R 4C/4S are distal from the E6/peptide interface (Supplemental Fig. 3C).

In both LxxLL-bound E6 proteins, the two zinc-binding domains are joined by a linker helix (Fig. 1 and Supplemental Fig. 4). While the BPV1 and HPV16 E6C domains have a similar fold, the two E6N domains have structurally resolved regions that are essentially superposable but differ in their N-terminal regions (Supplemental Fig. 3B and 4). Indeed, the sequence of HPV16 E6N includes an N-terminal extension that is absent in BPV1 E6N (Supplemental Fig. 9). In addition, the first 10 residues of BPV1 E6N are not visible in the electron density map.

The E6-bound LxxLL motifs of both paxillin ($M_1D_2D_3L_4D_5A_6L_7L_8A_9D_{10}$) and E6AP ($E_1L_2T_3L_4Q_5E_6L_7L_8G_9E_{10}E_{11}R_{12}$) adopt a α-helical conformation from residues 1 to 8 (Fig. 1 and 2). Both motifs are inserted within a deep pocket formed by the two zinc-binding domains and the linker helix of E6 (Fig. 1A–B). By contrast, previously solved complexes of cellular FAT, CH and LBD domains bound to LxxLL motifs (24–26) all showed the helical motif interacting with a shallow surface of the domain (Fig. 1C).

The three leucine residues (L_4, L_7 and L_8) of the motif are accommodated within a hydrophobic cavity mostly contributed by the E6N domain and linker helix (Fig. 1B, 2B, 2D and Supplemental Fig. 9). Point mutations altering hydrophobic residues of the cavity (i.e. F37S, L58S in BPV1 E6 and L50E in HPV16 E6) decrease both LxxLL peptide binding and

E6 transformation (BPV1 E6/paxillin) or p53 degradation (HPV16 E6/E6AP) activities (Fig. 3 and Supplemental Fig. 8A).

Surrounding the hydrophobic cavity, a positively charged surface (Supplemental Fig. 5), favorable to the acidic moieties of the peptide, includes a number of arginine residues that play specific roles in the architecture of the complex. The side-chain of a strictly conserved arginine (R89 in BPV1 and R102 in HPV16) holds together, like a keystone, the E6C domain, the E6N domain and the peptide by interacting with L_8 of the peptide and with main chain atoms at the C-termini of both E6N α1 helix and the peptide's helix. (Fig. 2).

Adjacent to R89/R102, BPV1 R121 and HPV16 R131 provide structurally equivalent contacts to backbone and side chains moieties of the peptide (Fig. 2). Free energy decomposition analysis (27) coupled to prior molecular dynamics (MD) simulations of the complexes revealed favorable van der Waals terms for arginine residues of BPV1 E6 R89 and R121 and of HPV16 E6 R102 and R131 (Supplemental Fig. 6) that are consistent with their multiple interactions at the complex interface. Mutagenesis of all these arginine residues markedly decreased peptide binding and biological activities of the two E6 proteins (Fig. 3 and Supplemental Fig. 8).

A number of peripheral E6 arginine side-chains selectively clamp acidic and/or polar side-chains of the LxxLL peptide (Fig. 2). In BPV1 E6, R42 and R116 interact with D_3 and D_5, respectively (Fig. 2A). In HPV16 E6, R55 (equivalent to BPV1 R42) interacts with T_3 and E_6. R129 (equivalent to BPV1 R116) displays conformational disorder in the crystal (Supplemental Fig. 6A), where it is oriented away from the peptide towards MBP (Fig. 2C and Supplemental Fig. 7A). However, upon MD simulation of the E6/E6AP complex devoid of MBP, the side-chain of R129 readily reorients to form a direct interaction with residue E_1 of the E6AP peptide (Supplemental Fig. 7B–C). In HPV16 E6, R10 at the N-terminus of E6N forms an additional ion bridge with E_{11} of the C-terminus of the target peptide (Fig. 2C). Alanine mutagenesis of these peripheral arginine residues had little or no influence on peptide binding or the tested biological activities with the exception of BPV1 R116, whose mutation markedly decreased paxillin binding and cellular transformation (Fig. 3 and Supplemental Fig. 8). Indeed, the side-chain of R116 is involved in a network of direct or-water mediated polar interactions at the E6C/peptide interface and in cation–π stacking with the aromatic side-chain of W65 (Fig. 2A and Supplemental Fig. 7C). This environment appears to strongly stabilize the R116-D_5 salt bridge, as confirmed by the high electrostatic free energy term displayed by both R116 and D_5 (Supplemental Fig. 6A).

A salient difference between the two structures concerns the mode of recognition of the N-terminus of the bound peptide, which is exclusively hydrophobic for paxillin and purely electrostatic for E6AP (Supplemental Fig. 6). Indeed, in the BPV1 E6/paxillin complex, M_1 of paxillin interacts with a hydrophobic patch at the C-terminus of the linker helix constituted by W65 and L64 (Fig. 2A and Supplemental Fig. 7C). In HPV16 E6, E6 residues L64 and W65 are substituted by basic residues R77 and H78, which together with R129 form a favorable electrostatic environment for the interaction with E_1 of the E6AP peptide (Fig. 2C and Supplemental Fig. 7C).

Many cellular functions are mediated by short linear interaction motifs (SLIMs), whose simple and redundant sequences constitute an Achille's heel for viral attack (28). Whereas viral proteins very often contain mimics of cellular SLIMs (28), E6 has an original fold that captures cellular acidic LxxLL motifs. In contrast to cellular proteins, which recruit LxxLL motifs on shallow surfaces of globular helical domains (24, 25), E6 captures these motifs within a binding pocket composed of three structural modules (Fig. 1). LxxLL-contacting residues are located at equivalent positions in HPV16 and BPV1 E6 sequences, and these

positions are generally conserved (Supplemental Fig. 9) suggesting that all mammalian E6 proteins contain a LxxLL-binding pocket. Furthermore, BPV1 and HPV16 E6 mutants disrupted for LxxLL-motif binding systematically lost transformation and degradation activities (Fig. 3), indicating that the conserved LxxLL-binding pocket is essential to the tumorigenic phenotype of E6 proteins. This pocket thus represents a promising target for therapeutic drugs.

E6 peptide-contacting residues play distinct roles. Hydrophobic pocket residues as well as the “keystone” arginine R89/R102 only establish contacts with the invariable leucine side chains of the motif and/or sequence-independent contacts with the peptide backbone. Other E6 residues function as “readers”, which discriminate variations of the LxxLL motif through sequence-dependent contacts to variable side chains of the peptide. In particular the nature of residues located at the C-terminus of the E6 linker helix or at the N-terminus of E6N domain may influence the selection of residues at the N- or C-terminus of the peptide, respectively. Conversely, some reader residues may tolerate variations in the position of key acidic residues in the LxxLL motif sequence, as equivalent arginine residues in BPV1 E6 and HPV16 E6 can interact with acidic side chains belonging to different turns of the peptide helix (Fig. 2). Such combinations of discriminative and tolerant reading mechanisms should allow different E6 proteins to capture different panels of host proteins bearing variations of the LxxLL motif.

In the absence of target peptide, E6 is likely to adopt a different overall structure, since the few interactions connecting the E6N, linker helix and E6C modules (Supplemental Fig. 10) are likely insufficient to maintain the E6 architecture observed in the complex structures. The propensity for self-association (21) and the strong affinity for target motifs (23, 29, 30) suggest that most E6 molecules preferentially exist as target-bound complexes in infected cells.

The data suggest that different modes of interaction can co-exist on one single molecule of E6. The LxxLL binding region, the PDZ domain binding motif at the extreme C-terminus of E6 (31, 32) and the E6N self-association interface required for p53 degradation (19) do not overlap when they are mapped onto the structure of HPV16 E6 (Fig. 4). Solvent accessible surfaces not involved in these three interactions represent candidate E6 regions for p53 binding. Structural studies of E6 in complex with multiple partners are now required, to decipher the mechanisms of E6 oncogenic activities such as the degradation of host target proteins.

Supplementary Material

Refer to Web version on PubMed Central for supplementary material.

Acknowledgments

This work was supported by institutional support from CNRS, Université de Strasbourg, INSERM, the European Commission SPINE2-Complexes project (contract n° LSHG-CT-2006-031220) and grants from ARC (n° 3171), ANR (ANR-MIME-2007 EPI-HPV-3D) and NIH (grant R01CA134737). S.C. was supported by ANR, A.o.M.o.S. by ARC and K.o.B. by College Doctoral Européen. S.V.P, N.B, and T.A. were supported by NIH grants (CA120352, CA134737 and CA08093) to S.V.P and institutional support from the University of Virginia. S.C., K.o.B. and M.G.F. were supported by NIH grant CA134737. MD calculations were performed at the Mèso-Centre of the University of Strasbourg. The authors thank members of the ESRF-EMBL joint Structural Biology groups for the use of beamline facilities and for help during data collection, members of the IGBMC common services for assistance, and Bruno Kieffer, Annick Dejaegere as well as all members of the “Oncoproteins” team for helpful discussions and advice. Coordinates and structure factors have been deposited at the Protein Data Bank with accession codes 3PY7 and 4GIZ.

References and Notes

1. Bernard HU, et al. Classification of papillomaviruses (PVs) based on 189 PV types and proposal of taxonomic amendments. Virology. 2010; 401:70. [PubMed: 20206957]
2. zur Hausen H. Immortalization of human cells and their malignant conversion by high risk human papillomavirus genotypes. Semin Cancer Biol. 1999; 9:405. [PubMed: 10712887]
3. Pfister H, et al. High prevalence of epidermodysplasia verruciformis-associated human papillomavirus DNA in actinic keratoses of the immunocompetent population. Arch Dermatol Res. 2003; 295:273. [PubMed: 14618345]
4. Nasir L, Campo MS. Bovine papillomaviruses: their role in the aetiology of cutaneous tumours of bovids and equids. Vet Dermatol. 2008; 19:243. [PubMed: 18927950]
5. Huibregtse JM, Scheffner M, Howley PM. A cellular protein mediates association of p53 with the E6 oncoprotein of human papillomavirus types 16 or 18. EMBO J. 1991; 10:4129. [PubMed: 1661671]
6. Scheffner M, Werness BA, Huibregtse JM, Levine AJ, Howley PM. The E6 oncoprotein encoded by human papillomavirus types 16 and 18 promotes the degradation of p53. Cell. 1990; 63:1129. [PubMed: 2175676]
7. Tungteakkhun SS, Duerksen-Hughes PJ. Cellular binding partners of the human papillomavirus E6 protein. Arch Virol. 2008; 153:397. [PubMed: 18172569]
8. Rozenblatt-Rosen O, et al. Interpreting cancer genomes using systematic host network perturbations by tumour virus proteins. Nature. 2012; 487:491. [PubMed: 22810586]
9. Ronco LV, Karpova AY, Vidal M, Howley PM. Human papillomavirus 16 E6 oncoprotein binds to interferon regulatory factor-3 and inhibits its transcriptional activity. Genes Dev. 1998; 12:2061. [PubMed: 9649509]
10. Brimer N, Lyons C, Wallberg AE, Vande Pol SB. Cutaneous papillomavirus E6 oncoproteins associate with MAML1 to repress transactivation and NOTCH signaling. Oncogene. 2012; 31:4639. [PubMed: 22249263]
11. Tan MJ, et al. Cutaneous beta-human papillomavirus E6 proteins bind Mastermind-like coactivators and repress Notch signaling. Proc Natl Acad Sci U S A. 2012; 109:E1473. [PubMed: 22547818]
12. Huibregtse JM, Scheffner M, Howley PM. Localization of the E6-AP regions that direct human papillomavirus E6 binding, association with p53, and ubiquitination of associated proteins. Mol Cell Biol. 1993; 13:4918. [PubMed: 8393140]
13. Chen JJ, Hong Y, Rustamzadeh E, Baleja JD, Androphy EJ. Identification of an alpha helical motif sufficient for association with papillomavirus. J Biol Chem. 1998; 273:13537. [PubMed: 9593689]
14. Tumbarello DA, Brown MC, Turner CE. The paxillin LD motifs. FEBS Lett. 2002; 513:114. [PubMed: 11911889]
15. Vande Pol SB, Brown MC, Turner CE. Association of Bovine Papillomavirus Type 1 E6 oncoprotein with the focal adhesion protein paxillin through a conserved protein interaction motif. Oncogene. 1998; 16:43. [PubMed: 9467941]
16. Tong X, Howley PM. The bovine papillomavirus E6 oncoprotein interacts with paxillin and disrupts the actin cytoskeleton. Proc Natl Acad Sci U S A. 1997; 94:4412. [PubMed: 9114003]
17. Wade R, Brimer N, Vande Pol S. Transformation by bovine papillomavirus type 1 E6 requires paxillin. J Virol. 2008; 82:5962. [PubMed: 18385245]
18. Thomas M, et al. Human papillomaviruses, cervical cancer and cell polarity. Oncogene. 2008; 27:7018. [PubMed: 19029942]
19. Zanier K, et al. Solution structure analysis of the HPV16 E6 oncoprotein reveals a self-association mechanism required for E6-mediated degradation of p53. Structure. 2012; 20:604. [PubMed: 22483108]
20. Nomine Y, et al. Structural and functional analysis of E6 oncoprotein: insights in the molecular pathways of human papillomavirus-mediated pathogenesis. Mol Cell. 2006; 21:665. [PubMed: 16507364]
21. Zanier K, et al. E6 proteins from diverse papillomaviruses self-associate both in vitro and in vivo. J Mol Biol. 2010; 396:90. [PubMed: 19917295]

22. Materials and methods are available as supplementary materials on *Science* Online.
23. Sidi AO, et al. Strategies for bacterial expression of protein-peptide complexes: application to solubilization of papillomavirus E6. Protein Expr Purif. 2011; 80:8. [PubMed: 21777678]
24. Hoellerer MK, et al. Molecular recognition of paxillin LD motifs by the focal adhesion targeting domain. Structure. 2003; 11:1207. [PubMed: 14527389]
25. Lorenz S, et al. Structural analysis of the interactions between paxillin LD motifs and alpha-parvin. Structure. 2008; 16:1521. [PubMed: 18940607]
26. Shiau AK, et al. The structural basis of estrogen receptor/coactivator recognition and the antagonism of this interaction by tamoxifen. Cell. 1998; 95:927. [PubMed: 9875847]
27. Lafont V, Schaefer M, Stote RH, Altschuh D, Dejaegere A. Protein-protein recognition and interaction hot spots in an antigen-antibody complex: free energy decomposition identifies “efficient amino acids”. Proteins. 2007; 67:418. [PubMed: 17256770]
28. Davey NE, Trave G, Gibson TJ. How viruses hijack cell regulation. Trends Biochem Sci. 2011; 36:159. [PubMed: 21146412]
29. Zanier K, et al. Kinetic analysis of the interactions of Human Papillomavirus E6 oncoproteins with the ubiquitin ligase E6AP using Surface Plasmon Resonance. J Mol Biol. 2005; 349:401. [PubMed: 15890204]
30. Sekaric P, Cherry JJ, Androphy EJ. Binding of human papillomavirus type 16 E6 to E6AP is not required for activation of hTERT. J Virol. 2008; 82:71. [PubMed: 17942561]
31. Charbonnier S, et al. The structural and dynamic response of MAGI-1 PDZ1 with noncanonical domain boundaries to the binding of human papillomavirus E6. J Mol Biol. 2011; 406:745. [PubMed: 21238461]
32. Zhang Y, Dasgupta J, Ma RZ, Banks L, Thomas M, Chen XS. Structures of a human papillomavirus (HPV) E6 polypeptide bound to MAGUK proteins: mechanisms of targeting tumor suppressors by a high-risk HPV oncoprotein. J Virol. 2007; 81:3618. [PubMed: 17267502]
33. Das K, Bohl J, Vande Pol SB. Identification of a second transforming function in bovine papillomavirus type1 E6 and the role of E6 interactions with paxillin, E6BP, and E6AP. J Virol. 2000; 74:812. [PubMed: 10623743]
34. Ned R, Allen S, Vande Pol S. Transformation by bovine papillomavirus type 1 E6 is independent of transcriptional activation by E6. J Virol. 1997; 71:4866. [PubMed: 9151888]

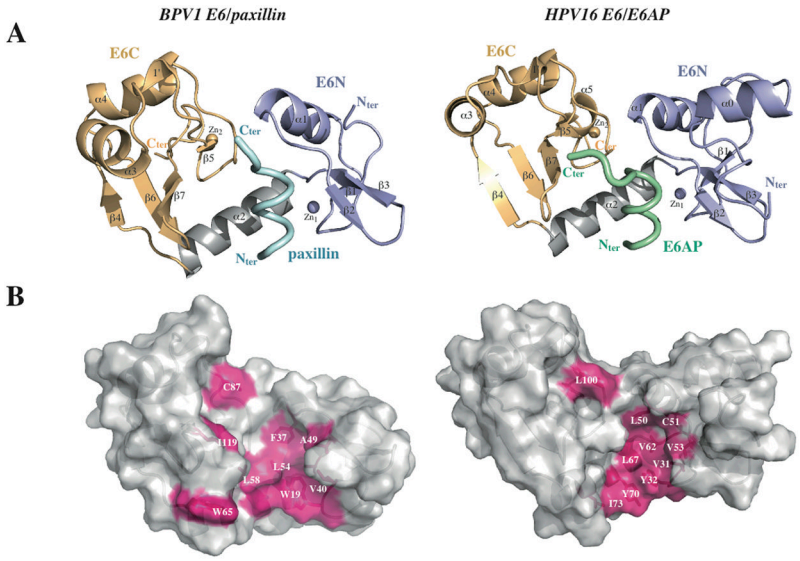

Fig. 1.

X-ray structures of E6/LxxLL complexes. (**A**) The structures of BPV1 E6 bound to residues 1–10 of paxillin (*left panel*) and of HPV16 E6 bound to residues 403–414 of E6AP (*right panel*). violet: E6N; grey: linker helix; gold: E6C; cyan/green: LxxLL peptides. (**B**) The hydrophobic pocket (pink) responsible for LxxLL motif recognition in BPV1 E6 (*left panel*) and HPV16 E6 (*right panel*). These structures show helical LxxLL peptides inserted in a deep pocket formed by the two domains, unlike other cellular domains (FAT, CH and LBD) interacting through shallow surfaces with the cognate LxxLL peptides. See also Supplementary Fig. 5.

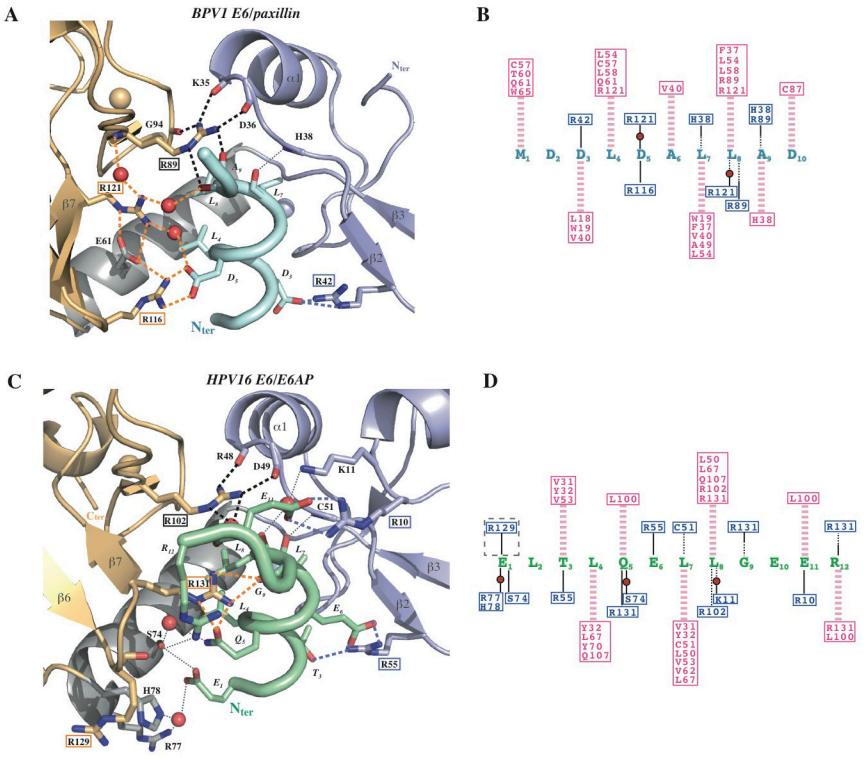

Fig. 2.

Networks of E6/LxxLL peptide interactions. (**A**) Polar interactions between BPV1 E6 and paxillin. Red spheres: water molecules; black dashed lines: interactions mediated by "keystone" arginine R89; violet/orange dashed lines: intermolecular interactions mediated by E6N/E6C arginines; dotted lines: other polar interactions. (**B**) All contacts between BPV1 E6 and paxillin. Pink dashed lines: hydrophobic contacts; black lines: polar contacts mediated by side chain (continuous lines) or main chain (dotted lines); pink/blue boxed residues: E6 hydrophobic/polar contributors; E6 polar residues displaying favorable van der Waals terms (ΔE^{vdw}< -1 kcal/mol, Supplemental Fig. 6A) are included as hydrophobic contributors. (**C**) Polar interactions between HPV16 E6 and E6AP. Black dashed lines: interactions mediated by "keystone" arginine R102; violet/orange dashed lines: intermolecular interactions mediated by E6N/E6C arginines. **(D**) All contacts between HPV16 E6 and E6AP. R129-E_1 (dashed gray line) is deduced from MD simulations (Supplemental Fig. 7).

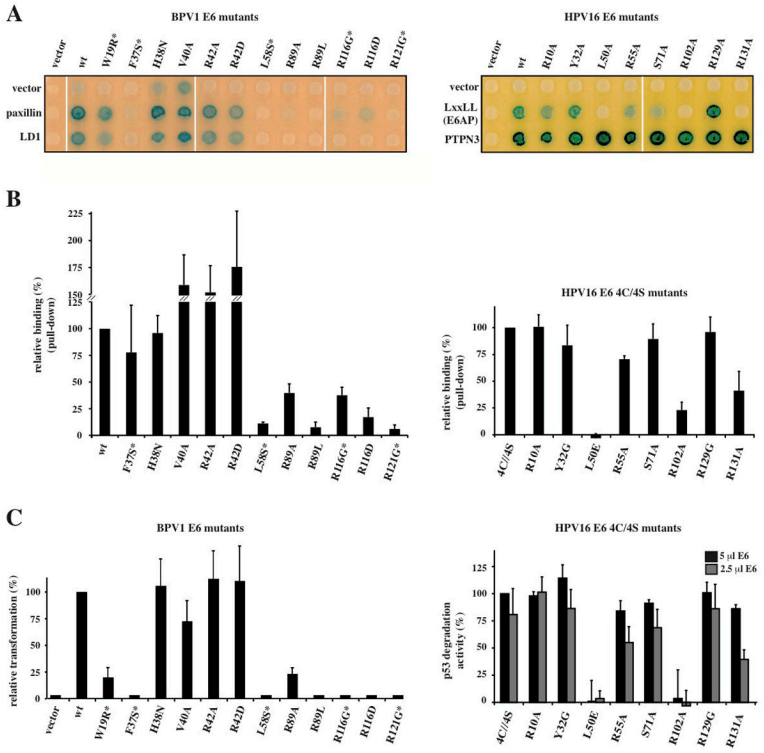

Fig. 3.

LxxLL binding and functional activities of E6 mutants. (**A**) Yeast two-hybrid analysis of BPV1 E6 *(left panel)* and HPV16 E6 *(right panel)* mutants binding to paxillin (full-length or LD1 peptide) and E6AP peptide respectively. PTPN3 (targeting the PDZ binding motif) is included as control of HPV16 E6 expression. (**B**) Pull-down assays of BPV1 E6 *(left panel)* and HPV16 E6 *(right panel)* mutants binding to GST-fused LxxLL peptides. The data (mean ± sd) were normalized to 100% for the reference protein. "*": previously investigated mutants (15, 33, 34). HPV16 E6 mutations were introduced in the E6 4C/4S construct. (**C**) Oncogenic activities of E6 mutants. The data (mean ± sd) were normalized to 100% for the reference protein. (*Left panel*) Transformation phenotypes of BPV1 E6 mutants, quantified using numbers of anchorage-independent colonies. (*Right panel)* p53 degradation activities of HPV16 E6 mutants measured by incubating constant amounts of p53 with either 2.5 or 5 µl of E6 translation product. I_0 and I correspond to, respectively, the p53 signal before and after incubation with E6. See also Supplemental Fig. 8.

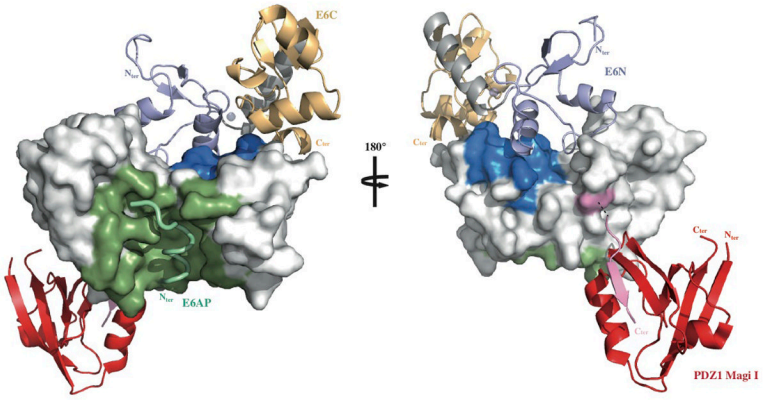

Fig. 4.

Mapping HPV16 E6 functional regions. The different binding sites of HPV16 E6 map to distinct regions of the protein's solvent accessible surface. LxxLL binding and E6 self-association residues are colored green and blue respectively. The position of the second E6 molecule shown in the ribbon representation was modeled based on the geometry of the E6N homodimer interface (2LJY.pdb). The C-terminal PDZ binding motif (pink) is disordered in the NMR structure of the isolated HPV16 E6C domain and adopts a β-strand conformation upon binding to the PDZ1 of Magi I (red) (2KPL.pdb). The relative orientation of E6 and the PDZ domain shown is arbitrary. Surfaces colored white are potentially available for binding to p53. See also Supplemental Fig. 9.